Ergod. Th. & Dynam. Sys. (2014), **34**, 211–235 © *Cambridge University Press, 2012*
doi:10.1017/etds.2012.132

Templates for geodesic flows

TALI PINSKY†

The Technion, Israeli Institute of Technology, Mathematics Department, Haifa 32000, Israel (e-mail: otali@tx.technion.ac.il)

(*Received* 14 *September* 2011 *and accepted in revised form* 9 *August* 2012)

Abstract. We construct templates for geodesic flows on an infinite family of Hecke triangle groups. Our results generalize those of E. Ghys [Knots and dynamics. *Proc. Int. Congress of Mathematicians*. Vol. 1. International Congress of Mathematicians, Zürich, 2007], who constructed a template for the modular flow in the complement of the trefoil knot in S^3. A significant difficulty that arises in any attempt to go beyond the modular flow is the fact that for other Hecke triangles the geodesic flow cannot be viewed as a flow in S^3, and one is led to consider embeddings into lens spaces. Our final result is an explicit description of a single 'Hecke template' which contains all other templates we construct, allowing a topological study of the periodic orbits of different Hecke triangle groups all at once.

1. *Introduction*

1.1. *Motivation.* The study of periodic orbits in dynamical systems is a basic problem with a long history. In a variety of examples one would like to find periodic orbits, and to study their properties and general structure. This is of great importance, for instance, in taking the semi-classical limit of dynamical systems [**1**], or for computing averages of observables in both classical and quantum chaotic systems [**5**].

We are interested in the case of flows in three-dimensional manifolds. A periodic orbit of such a flow is an embedding of S^1 into the 3-manifold, hence a knot, and one can ask which knot types arise as periodic orbits for a certain flow, or what knot invariants (if any) they share.

This problem was considered by Birman and Williams in [**3, 4**]. The first example Birman and Williams analyzed is the flow associated with the famous Lorenz equations. Here it was shown that the family of knots arising as periodic orbits, the so-called 'Lorenz knots', has very special properties. As an example of their results we mention that Lorenz knots are prime and every Lorenz link is a fibered link, and a positive braid. These results are based on the fact that all periodic orbits of the Lorenz flow are described by a simple

† Current address: Department of Mathematics, UBC, 1984 Mathematics Road, Vancouver, BC, Canada V6T 1Z2.

https://doi.org/10.1017/etds.2012.132 Published online by Cambridge University Press

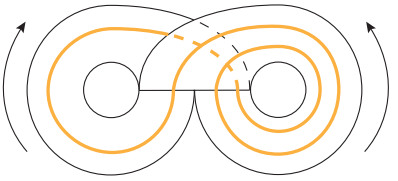


FIGURE 1. The Lorenz template and a periodic orbit.

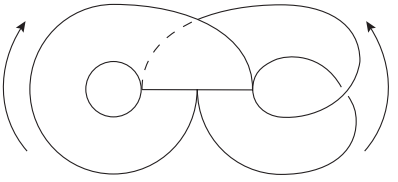


FIGURE 2. A universal Lorenz-like template.

combinatorial construction, called the template. The Lorenz template is given in Figure 1, together with a typical periodic orbit. All periodic orbits of the equations arise as orbits in the Lorenz template.

A second example considered by Birman and Williams is the suspension flow on the complement of the figure eight knot in S^3. They have also constructed a template for the periodic orbits of this system. But, remarkably, here it was shown by Ghrist [**9**] that the template is in fact a universal template: every possible knot in S^3 arises as a periodic orbit of this flow, without exception. In the same paper Ghrist showed that some templates termed Lorenz-like, studied before by Sullivan (see, for example, [**17, 18**]), are also universal. In particular, even one half twist in one of the ears of the Lorenz template gives rise to a universal template (see Figure 2).

Thus, constructing a template for a given flow has far-reaching consequences in the study of knot types arising as periodic orbits, enabling a description of their knot invariants, or a proof of their universality. For this it is necessary to obtain a complete description of the template, since even seemingly minute changes in the template type can dramatically affect the properties of the knots produced by the template.

In the important case of hyperbolic flows Birman and Williams have proved that a template always exists [**4**], but its explicit construction has been done in very few specific cases. Even within the well-studied class of hyperbolic flows consisting of geodesic flows on the unit tangent bundle of surfaces of constant negative curvature, the first construction of a template was achieved only recently, for the modular surface. Namely, Ghys [**10**] established the extraordinary fact that the modular template coincides with the Lorenz template. In particular, this fact implies that the modular knots share the special properties of the Lorenz knots mentioned above. For further study of the modular knots, see [**6**].

We were very much inspired by Ghys' work, which raises many interesting questions. One such compelling problem is to understand which properties of the periodic orbits of the modular surface (if any) hold for the periodic orbits of the geodesic flows on other surfaces. A first step in the solution of this problem is constructing templates for these flows, and this will be our goal in the present paper.

https://doi.org/10.1017/etds.2012.132 Published online by Cambridge University Press



FIGURE 3. The template constructed for the (2, 5) case.

1.2. *Description of results.* We will focus on a class of surfaces which form a natural generalization of the modular surface, namely the class of orbifolds with two cone points of orders 2 and k and one cusp, with k odd. The modular surface appears as the first member of this family, with $k = 3$. Alternatively, the surfaces in question arise as $\mathbb{H}^2/\Gamma(2, k)$ where $\Gamma(2, k)$ is the Hecke triangle group associated with the triangle $(2, k, \infty)$.

We will give a complete description of the template for the geodesic flow on the unit tangent bundles of these surfaces. Consideration of orbifolds with a cone point of arbitrary order gives rise to significant new phenomena. As already noted the unit tangent bundle of the modular surface can be identified with the complement of the trefoil knot in S^3. For all other surfaces in our class, the unit tangent bundle is identified with the complement of a knot ξ in a non-trivial lens space $L(p, q)$. As $L(p, q)$ is a quotient of S^3 by a $\mathbb{Z}_p$ action, ξ has a natural lift to S^3. This lift equals the $(2, k)$ torus knot, generalizing the $(2, 3)$ case of the modular surface. We note that the lens space in question is not determined uniquely, and in fact the unit tangent bundle of each $(2, k)$ orbifold (including for $k = 3$) embeds into a specific countable family of lens spaces, whose parameters are given as explicit functions of the Euler number of the bundle and k.

The templates we construct are those arising for Euler number zero. For the case of the $(2, 5)$ orbifold, for example, see Figure 3. Its embedding into $L(3, 1)$ will be explained in the following sections.

We expect to use these templates to prove that all the periodic orbits on these templates are prime in the 3-manifolds resulting from the unit tangent bundles by Dehn filling the cusp [**13**]. Note that the template contains the Lorenz template as a subtemplate, as will be the case for the templates we construct for the $(2, k)$ orbifolds. Thus, the templates we construct are extensions of the basic Lorenz template, but only due to the specific choice of Euler number zero. Other choices of non-zero Euler number will not give rise to a subtemplate with two unlinked ears each of whose core is the unknot.

Going back to the case of the modular surface, we note that here too a countable family of lens spaces is obtained in our construction, and it is a remarkable fact that the choice of Euler number zero is the choice producing the Lorenz template, and at the same time is the only one which gives the lens space S^3.

We note that the periodic orbits of the geodesic flow on any (n, k) Hecke triangle were recently considered by Dehornoy [**7**]. One of his results is that any two periodic orbits

https://doi.org/10.1017/etds.2012.132 Published online by Cambridge University Press

in any of these systems are negatively linked with each other, thus all these flows are 'left-handed'.

Remark. The description of the geodesic flow on the modular surface as a flow in the complement of the trefoil knot in S^3, together with the identification of the modular knots as Lorenz knots, poses the following intriguing question. Is it possible to identify a Lorenz-invariant trefoil knot, in the complement of which the Lorenz flow takes place? We believe this is indeed the case, and specifically that the invariant curves connecting the fixed points of the Lorenz flow form a trefoil. We refer to [**2, 11**] for further discussion of this matter.

Organization of the paper. The paper is organized as follows. In §2 we introduce some preliminaries regarding hyperbolic geometry. In §3, after some preliminaries on lens spaces and Seifert fibered spaces, we discuss the possible embeddings of the unit tangent bundle into lens spaces. In §4 we briefly describe the theory of templates and then construct templates for the geodesic flows on the $(2, k)$ orbifolds. In §5 we construct a single template containing all $(2, k)$ templates as subtemplates.

2. *Hyperbolic geometry*

2.1. *Hyperbolic unit tangent bundles.* Let $\mathbb{H}$ be the hyperbolic plane. The tangent bundle $T_p\mathbb{H}$ at any point $p \in \mathbb{H}$ is $\mathbb{R}_2$. Now let $UT\mathbb{H}$ be the unit tangent bundle of $\mathbb{H}$, with fiber at each point consisting of all vectors of norm 1, that is, S^1. We call the fiber over a point the circle of directions at that point. As $\mathbb{H}$ is simply connected $UT\mathbb{H}$ is a trivial bundle, and can be described as the set of pointers (p, θ) where $p \in \mathbb{H}$ and $0 \le \theta < 2\pi$ is an angle representing the unit vector $e^{\theta i} \in S^1$ in the plane $T_p\mathbb{H}$. Recall that $\mathrm{Isom}_+(\mathbb{H}) \cong \mathrm{PSL}_2(\mathbb{R})$, and the stabilizer $St(x) \subset \mathrm{PSL}_2(\mathbb{R})$ of a point $x \in \mathbb{H}$ consists of all rotations about x. $St(x)$ is thus naturally identified with the S^1 fiber above x in $UT\mathbb{H}$, and, in particular, $\mathrm{PSL}_2(\mathbb{R}) \cong UT\mathbb{H}$.

Any differentiable path $\gamma(t)$ in $\mathbb{H}$ has a natural lift to $UT\mathbb{H}$, by $\gamma(t) \mapsto \tilde{\gamma}(t) = (\gamma(t), \dot{\gamma}(t)/\|\dot{\gamma}(t)\|)$. Let $\gamma(t)$ and $\delta(t)$ be two differentiable paths, isotopic by $h_s(t)$. The isotopy may induce an isotopy between $\tilde{\gamma}(t)$ and $\tilde{\delta}(t)$, if for any fixed s, $h_s(t)$ is differentiable, and the lifted paths $\tilde{h}_s(t)$ are continuously deformed one to the other along s. In this case the isotopy is called a *regular isotopy*, and can be considered to be an isotopy in $UT\mathbb{H}$.

2.2. *The geodesic flow on $UT\mathbb{H}$.* The geodesic flow $\hat{\phi}_t$ on $\mathbb{H}$ is defined as the flow taking a pointer in $UT\mathbb{H}$ by parallel transport along the unique geodesic in $\mathbb{H}$ passing through it, a distance t.

Let us define for any $t \in \mathbb{R}$, $G_t = \begin{pmatrix} e^{t/2} & 0 \\ 0 & e^{-t/2} \end{pmatrix}$. $\hat{\phi}_t$ is conjugated by g defined above to a flow on $\mathrm{PSL}_2(\mathbb{R})$, given by $\phi_t(B) \mapsto G_t B$.

Now, for any pointer in $UT\mathbb{H}$ we can consider a horocycle corresponding to the endpoint of the geodesic it defines, h^-, and the horocycle corresponding to the geodesic's starting point, h^+. We consider these horocycles in the unit tangent bundle, for h^- with all directions pointing toward the endpoint, and for h^+ with all directions pointing away from the starting point, as in Figure 4.

https://doi.org/10.1017/etds.2012.132 Published online by Cambridge University Press

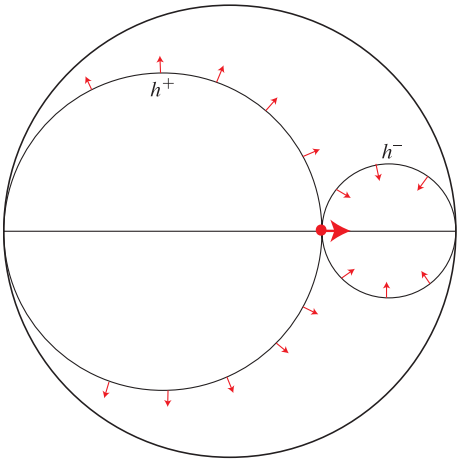


FIGURE 4. The stable and unstable manifolds for the geodesic flow in $\mathbb{H}$.

The one-parameter group $H_s^- = \left(\begin{smallmatrix} 1 & 0 \\ s & 1 \end{smallmatrix}\right)$ defines the flow along the horocycle h^-, and the one-parameter group $H_u^+ = \left(\begin{smallmatrix} 1 & u \\ 0 & 1 \end{smallmatrix}\right)$ along h^+. As $G_t H_s^- G_t^{-1} = H_{se^{-t}}^-$, we see that the images of points on the horocycle h_- approach each other under the geodesic flow exponentially fast. In the same manner, $G_t H_u^+ G_t^{-1} = H_{ue^t}^+$ and so points on h^+ diverge exponentially fast under the geodesic flow. We also note that the geodesic and the two horocycles through a point p in $UT\mathbb{H}$ are transversal, as can be seen in Figure 4, thus they constitute a basis for $T_p\mathbb{H}$.

2.3. *The unit tangent bundle of an orbifold.* Let $\mathcal{O}$ be an orbifold of dimension n. We will use only the case of dimension two, but the definitions are the same for any dimension. Take an orbifold atlas for $\mathcal{O}$. Each chart in the atlas is of the form $(U_i/G_i, \psi_i)$, where each U_i is an open subset of $\mathbb{R}^n$, and G_i is a finite group acting linearly and faithfully on $\mathbb{R}^n$.

The tangent bundle of $\mathcal{O}$ is the $2n$-dimensional orbifold defined by the charts $((U_i, \mathbb{R}^n)/G_i, \tilde{\psi}_i)$ where $g \in G_i$ acts by $g((p, v)) = (g(p), dg_p(v))$.

If $\mathcal{O}$ is a good orbifold, that is, a quotient of a manifold M by a properly discontinuous group action Γ, the tangent bundle $T\mathcal{O}$ is homeomorphic to $\Gamma\backslash TM$. For the full definitions, see [**12**, p. 92].

Let $\Gamma \subset \mathrm{PSL}_2(\mathbb{R})$ be a Fuchsian group acting on $\mathbb{H}$. The quotient $\Gamma\backslash\mathbb{H}$ is a two-dimensional orbifold. It inherits a hyperbolic structure from $\mathbb{H}$, and its tangent bundle is $\Gamma\backslash T\mathbb{H}$. In this case, it is possible to define also the unit tangent bundle $\Gamma\backslash UT\mathbb{H} \cong \Gamma\backslash \mathrm{PSL}_2(\mathbb{R})$, as the group acts by isometries. The geodesic flow on the unit tangent bundle is defined to be $\tilde{\phi}_t(B) \mapsto BH_t$, namely by projecting the flow ϕ_t defined above for $\mathrm{PSL}_2(\mathbb{R})$ via Γ.

2.4. *The (n, k) Hecke triangle group.* We now turn to the orbifolds which are the subject of our discussion. Consider the (n, k) Hecke triangle group $\Gamma_{(n,k)} := \langle v, u | v^k = u^n = e \rangle$. By considering as in [**10**] any two points of distance $d > 0$ in $\mathbb{H}$ and taking v to be a rotation

https://doi.org/10.1017/etds.2012.132 Published online by Cambridge University Press

of order $2\pi/k$ about the one and u a rotation of order $2\pi/n$ about the other, we arrive at a representation of $\Gamma_{(n,k)}$ into $\mathrm{PSL}_2(\mathbb{R})$. Any two representations corresponding to the same distance d are conjugate since the isometry group is distance transitive.

For any $n, k \in \mathbb{Z}$ there exists a distance d_0 for which the image of the representation is discrete, yet the orbifold $\Gamma\backslash\mathbb{H}$ is of finite volume. The representations for which the distance equals d_0 are called lattice representations of Γ and we denote the set of all such representations by $L(\Gamma)$. Denote the orbifold corresponding to any representation in $L(\Gamma)$ by $\mathcal{O}_{(n,k)}$. This orbifold has two cone points of order n and k and one cusp. For a distance $d > d_0$ the volume of the orbifold becomes infinite, that is, 'the cusp has opened'. Denote the orbifold corresponding to $d > d_0$ by $\mathcal{O}^d_{(n,k)}$.

A representation in $L(\Gamma)$ is determined by one pointer: a cone point in $\mathbb{H}$ of order k and any one of the k directions equally spaced along the circle of directions at that point, pointing to the neighboring n-cone points. We thus regard $L(\Gamma)$ as a set of pointers. Let us fix a representation $\Gamma_0 = (i, \pi/2) \in L(\Gamma)$. That is, Γ_0 has a k-cone point at i and an n-cone point at distance d_0 upwards along the imaginary axis. Γ_0 acts transitively on all k-cone points, and by rotations by $2\pi/k$ around i (and any other k-cone point), hence Γ_0 normalizes itself and $L(\Gamma) \cong \mathrm{PSL}_2(\mathbb{R})/\Gamma_0$. The following homeomorphisms $\mathrm{PSL}_2(\mathbb{R})/\Gamma_0 \cong \{\text{pointers in the plane}\}/\Gamma \cong UT\mathcal{O}_{(n,k)}$ also hold of course, as in §2.3.

We will use in the following the following homeomorphism:

$$h : \mathrm{PSL}_2(\mathbb{R})/\Gamma_0 \to L(\Gamma)$$
$$h : B \cdot \Gamma_0 \mapsto (B(i), dB_i(\pi/2)).$$

3. *The unit tangent bundle*

As noted in the introduction, the unit tangent bundle to the modular orbifold $\mathcal{O}_{(2,3)}$ is homeomorphic to the complement of a trefoil in S^3. This classical fact can be implemented for example by the Weierstrass invariants, and this was used by Ghys in [**10**] to compute the template of the modular flow. However, the fact that the unit tangent bundle is a subset of S^3 is in fact unique to the modular surface among the surfaces we consider, as we will see below.

In this section we will give a direct geometric description of the unit tangent bundle to $\mathcal{O}_{(n,k)}$ as a 3-manifold. We will subsequently describe the template for the geodesic flow embedded therein. We note, however, that the best one can attain for the general case is that for any orbifold $\mathcal{O}_{(n,k)}$, the unit tangent bundle has (infinitely many) embeddings into lens spaces. These are parameterized by the Euler number, and we will see later on that the choice of the embedding with Euler number zero gives rise to a template generalizing the Lorenz template.

This section is organized as follows. We begin in §§3.1 and 3.2 with brief reminders on lens spaces and Seifert fibered spaces, and in §3.3 we describe the structure of $UT\mathcal{O}_{(n,k)}$ as a Seifert fibered space. In §3.4 we define a certain vector field on the orbifolds $UT\mathcal{O}_{(2,k)}$. In §3.5 we parameterize the embeddings by the Euler number, and finally in §3.6 we describe explicitly the embeddings of $UT\mathcal{O}_{(2,k)}$ into the relevant lens spaces, given by the vector field.

https://doi.org/10.1017/etds.2012.132 Published online by Cambridge University Press

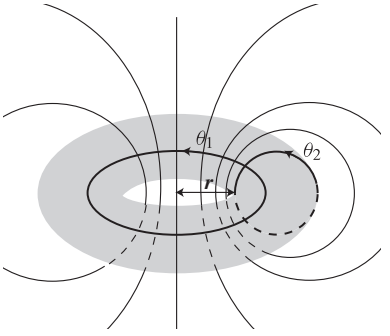


FIGURE 5. A fibration of S^3 by tori.

3.1. *Lens spaces.* The lens space $L(p, q)$, for integers $0 < q < p$, is defined to be the quotient of S^3 by the following action of $\mathbb{Z}_p$. Let S^3 be the vectors of norm 1 in $\mathbb{C}^2$; then any $w \in \mathbb{Z}_p$ acts by $w \cdot (z_1, z_2) = (w \cdot z_1, w^q \cdot z_2)$. This action is free, thus the resulting space $L(p \cdot q)$ is a compact three-dimensional manifold.

Another description of the same manifold is as follows. Let T_1 and T_2 be two solid tori. Fix a longitude and meridian generators l_i and m_i for $\pi_1(\partial T_i)$. Then choose an orientation-reversing homeomorphism $h : \partial T_1 \to \partial T_2$ so that $h_*(m_1) = pl_2 + qm_2$. Then the lens space $L(p, q)$ is given by gluing $T_1 \cup_h T_2$.

The homeomorphism between the two representations can be seen by a straightforward identification as follows. Consider the polar parameterization $(r_1, \theta_1, r_2, \theta_2)$ of $\mathbb{C}^2$. For a point in S^3, $r_1^2 + r_2^2 = 1$. This gives a parameterization (r, θ_1, θ_2) for S^3, where $r = r_1$, thus $0 \le r \le 1$, $0 \le \theta_1, \theta_2 < 2\pi$, with obvious identifications for $r = 1$ and $r = 0$. This is the well-known parameterization of S^3 by concentric tori sketched in Figure 5. The radii are invariant under the $\mathbb{Z}_p$ action and so r is invariant under the action, thus each of the tori is an invariant set. The action on each torus is given by

$$e^{2\pi mi/p} \cdot (r, \theta_1, \theta_2) \mapsto \left(r, \theta_1 + \frac{2\pi m}{p}, \theta_2 + \frac{2\pi mq}{p}\right).$$

Fix some $0 < r_0 < 1$. This gives a decomposition of S^3 to two solid tori. For the inner solid torus, that is, the union of tori $0 \le r \le r_0$, a meridian is given by $\theta_1 = 0$. As can be seen from the action, the quotient is the torus resulting from $0 < \theta_1 \le 2\pi/p$, by identifying the two disks in the boundary with a twist by $2\pi q/p$. Thus, $\theta_1 = 0$ remains a meridian for the quotient torus. This meridian is a longitude for the other torus in S^3, $r_0 < r \le 1$. The image of the longitude is a (p, q) curve in the quotient of the outer torus, and the equivalence of the definitions follows. See also [**14, 20**].

3.2. *Seifert fiber spaces.* In the section below we recall some terminology and facts about Seifert fiber spaces which can also be found in [**12, 15**].

Definition 3.1. An orientable 3-manifold is called a *Seifert fiber space* if it is a disjoint union of fibers homeomorphic to S^1, such that each fiber has a solid torus neighborhood, foliated by fibers which are not meridians for it.

https://doi.org/10.1017/etds.2012.132 Published online by Cambridge University Press

Definition 3.2. A *Seifert torus* of type (μ, ν), μ and ν coprime integers, is the torus obtained from a fibered cylinder $D^2 \times [0, 1]$ where the fibers are the lines $x \times [0, 1]$, by identifying $(x, 1)$ with $(r_{\nu/\mu}(x), 0)$ for every $x \in D^2$. $r_{\nu/\mu} : D^2 \to D^2$ is given by a rotation by angle $2\pi\nu/\mu$. Without loss of generality, we can assume that $\mu > 0$ and $0 \leq \nu \leq \frac{1}{2}\mu$.

For any boundary of a solid torus one has a basis for the homology consisting of a meridian (which is the element becoming trivial in the solid torus), and a longitude intersecting it once. For the boundary of a Seifert solid torus, one can also choose another basis, where the first element is chosen to be a fiber of the Seifert fibration, and the second element is any simple closed curve on the boundary which intersects the chosen fiber (and thus any fiber) only once. Such a curve is called a *crossing curve* and is defined up to adding any multiple of the fiber, as is the longitude in a meridian longitude pair.

Any fiber f in a general Seifert fiber space has a neighborhood homeomorphic to some Seifert torus, the homeomorphism taking f to the central fiber. The type of the Seifert torus is uniquely determined (taking the invariants normalized as in the theorem) and the fiber is called singular if $\nu \neq 0$. In a (μ, ν) fibered torus, any regular fiber f is homeomorphic to $(f_0)^\mu$, where f_0 is the singular fiber. This will be used later to identify the invariants of specific Seifert tori.

By identifying every fiber with a point one gets a map from any Seifert fiber space M to a two-dimensional orbifold S called the *orbit surface*. S cannot in general be embedded into M. Each cone point of S corresponds to a singular fiber of the Seifert fiber space. One can embed a subset of S into M in the following way. First, if M and S are closed, we remove a toral neighborhood of any regular fiber in M, and the corresponding disk in S, creating one boundary component J_0 for S. Then we remove a small neighborhood of each cone point of S, obtaining the *punctured orbit surface* of M we denote by S_0. Removing the corresponding toral neighborhoods of the singular fibers in M, we get a 3-manifold M_0 which is a bundle over S_0. Seifert [**15**] proves that S_0 can always be embedded into M_0, and the embedding is unique once the homology types of the boundary curves of S_0 on ∂M_0 are determined.

THEOREM 3.1. (Seifert) *Any closed Seifert fiber space is uniquely determined by invariants*

$$\{O/N, o/n, g, b; (\mu_1, \nu_1), \ldots, (\mu_s, \nu_s)\},$$

where one puts an O if M is orientable and N if not, and o if S is orientable, n if not. g is the genus of S, b is the Euler number of M. s is the number of the singular fibers, and a toral neighborhood of the singular fiber f_i, $1 \leq i \leq s$, is a Seifert torus of type (μ_i, ν_i).

Given the invariants, the space M can be constructed as follows. Begin with a surface of genus g with $s + 1$ punctures. This is homeomorphic to S_0. Take the trivial circle bundle over S_0, This is a fibered space with $s + 1$ toral boundary components. The boundary curves of S_0 on each of the boundary tori of M_0 are crossing curves for these tori. So for each boundary torus this determines a basis of a crossing curve c_i, $1 \leq i \leq s$, and a fiber f. Thus the invariants μ_i, ν_i for each singular torus uniquely determine a gluing of this singular torus to M_0 such that fibers match. Now there remains a single boundary

https://doi.org/10.1017/etds.2012.132 Published online by Cambridge University Press

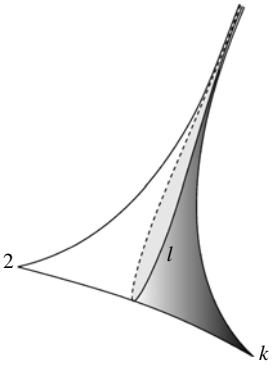


FIGURE 6. Divide $\mathcal{O}_{(2,k)}$ into two (singular) disks.

component, with a given crossing curve c_0. We glue in a (1, 0) fibered torus by gluing its meridian to a $c_0 - b \cdot f$ curve.

In the following we will consider open Seifert fiber spaces, having a single toral boundary. As by gluing in a Seifert torus one obtains a closed Seifert fiber space, it follows from Seifert's theorem that these manifolds are uniquely determined by the above invariants, excluding the Euler number b. b remains undetermined as the parameter determining the gluing, and parameterizes the countable set of closed Seifert fiber space into which the manifold can embed without adding singular fibers.

On each Seifert fiber space, one can define an S^1 action, moving each point along the fiber containing it. Consider the action on a neighborhood of a singular fiber, which is a (μ, ν) fibered torus. Take a meridional disk D for this torus, thus the torus is given by $D \times [0, 1]$ with the identification by a $2\pi\nu/\mu$ rotation. Choose a point x_0 on the meridian ∂D. There are μ intersection points of the orbit of x_0 (that is, the fiber containing x_0) with ∂D. We order these points as $x_0, \ldots, x_{\mu-1}$, by their order along the meridian. The flow takes $x_0 = x_0 \times 0$ along $[0, 1]$ to a point $x_0 \times 1$ identified under the rotation with x_ν. Thus, by knowing the action one can derive both μ (by the number of points in the orbit), and ν. This will be useful later on.

3.3. *The structure of the unit tangent bundle.*

THEOREM 3.2. *The unit tangent bundle to $\mathcal{O}_{(n,k)}$ is a Seifert fiber space consisting of two Seifert tori of invariants* $(k, 1)$ *and* $(n, 1)$.

Proof. We divide the proof into several steps.

Step 1. First we prove that the unit tangent bundle is a union of two Seifert tori. For this, divide the orbifold itself into two disks, each a neighborhood of one of the cone points, so that they intersect along a line as in Figure 6.

The unit tangent bundle to each of the disks is an S^1 bundle over the disk, that is, a fibered solid torus. It remains to prove that only one fiber in each torus is singular.

For a two-dimensional orbifold, a path making a small loop around a point together with the tangent direction at every point is isotopic to the fiber corresponding to that point (we

https://doi.org/10.1017/etds.2012.132 Published online by Cambridge University Press

orient both counterclockwise). Any two small loops on the surface are regularly isotopic, unless one of them encloses a cone point, hence all fibers except at the cone points are isotopic and the torus contains at most one singular fiber, the one corresponding to the cone point. We denote the singular fiber corresponding to the n-cone point by α and the one corresponding to the k-cone point by β.

As in §3.2, such a torus is determined up to homeomorphism by two natural numbers (μ, ν), $0 \leq \nu \leq \mu/2$. Denote the invariants of the torus which is the unit tangent bundle to a neighborhood of the n-cone point by (μ_n, ν_n), and the invariants of the other torus by (μ_k, ν_k). We now compute these invariants in two further steps.

Step 2. Computing μ_n and μ_k. Consider the universal covering space of the orbifold. This is a 2-plane and in it any two loops are isotopic. Hence, a lift of the singular fiber f_0 corresponding to the n-cone point (which projects to the singular fiber to the order n) and a lift of any of the regular fibers f are isotopic. Thus in the projection, $f \cong f_0^n$. In the same way, the k-singular fiber to the kth order is isotopic to a regular fiber. Hence as in §3.2, the two unit tangent bundles to the cone points' neighborhoods are two tori (k, ν_k) and (n, ν_n).

Step 3. Computing ν_n and ν_k. Following Montesinos [**12**], we consider the Seifert S^1 action on the unit tangent bundle, while viewing the unit tangent bundle as the representation variety of lattices.

The S^1 action, by the homeomorphism given in §2.4, is given by rotations of all lattices in the representation variety about i. Take a small neighborhood $B_\epsilon(i)$ of i in the plane (containing no other vertices of Γ_0). The set of lattice representations with a k-cone point within $B_\epsilon(i)$ is a toral neighborhood of the k-singular fiber. A meridional disk for this torus is the set of such lattices with (say) an upward direction (pointing to the nearest neighbor), and the set of such lattices with a cone point and an upward direction on the circle $S_\epsilon(i)$ is a meridian.

Fix a point $(x_0, \pi/2)$ on the meridian, and mark the k points equally spaced along $S_\epsilon(i)$ including x_0 by $\{x_0, x_1, \ldots, x_{k-1}\}$, ordered counterclockwise. The lattices corresponding to $\{(x_0, \pi/2), (x_1, \pi/2), \ldots, (x_{k-1}, \pi/2)\}$ are in the same S^1 orbit, and it is the order in which they are transformed to one another that determines ν_k, as in §3.2.

The rotation by $2\pi/k$ takes $(x_0, \pi/2)$ to $(x_1, \pi/2 + 2\pi/k) \sim (x_1, \pi/2)$. Hence $\nu_k = 1$, and in the same manner $\nu_n = 1$.

Concluding, the unit tangent bundle is the union of the Seifert tori $(k, 1)$ and $(n, 1)$. □

There is of course some identification on the boundaries of these two tori. This identification is addressed in the following theorem (compare with the results in [**19**]).

THEOREM 3.3. *The unit tangent bundle of $\mathcal{O}_{(n,k)}$ can be embedded in the lens space $L(n + k - nkc, 1 - nc)$ for any $c \in \mathbb{Z}$.*

Proof. Consider again the two disks into which $\mathcal{O}_{(n,k)}$ is divided in the previous proof, depicted in Figure 6. These disks intersect along a single (open) segment, denoted l, included in each of their boundaries. Consider the unit tangent bundles to each of the disks. These are two (fibered) solid tori, which each include the unit tangent bundle to l. This in turn is an annulus, contained in each of the boundary tori. By identifying the fibers

https://doi.org/10.1017/etds.2012.132 Published online by Cambridge University Press

lying above l with one another, one arrives at a gluing of the two tori $(k, 1)$ and $(n, 1)$ along an annulus. It is this gluing that yields the topology of $UT\mathcal{O}_{(n,k)}$. The annulus is a union of regular fibers (as all points on l are regular). Thus, the fiber above the same point on l is a regular fiber in each of the boundary tori. This yields that the gluing must identify a regular fiber on one boundary torus with a regular fiber on the other boundary torus.

Consider all orientation-reversing homeomorphisms between the boundary tori. Any such homeomorphism is given by matrix multiplication, by a matrix in $\mathrm{GL}(2, \mathbb{Z})$ with determinant -1. It is easy to compute that all such matrices satisfying the property that a $(n, 1)$ curve is glued to a $(k, 1)$ curve are

$$M_{n,k,c} = \begin{pmatrix} kc - 1 & n + k - nkc \\ c & 1 - nc \end{pmatrix}$$

for any $c \in \mathbb{Z}$. Two solid tori glued along their boundaries so that the meridian of one is glued to a (p, q) curve on the other results in the lens space $L(p, q)$, as in §3.1. Hence the unit tangent bundle can be embedded into any of the lens spaces $L(n + k - nkc, 1 - nc)$ as required. □

COROLLARY 3.4. *$UT\mathcal{O}_{(n,k)}$ can be embedded into S^3 if an only if $\{n, k\} = \{2, 3\}$, namely, for $\Gamma_{(2,3)} = \mathrm{PSL}_2(\mathbb{Z})$.*

Proof. First, the lens space $L(p, q)$ is homeomorphic to S^3 if and only if $p = \pm 1$. Indeed, recall that $L(0, 1) \cong S^2 \times S^1$, $L(p, q) \cong L(-p, q)$ and, for $p > 1$, $\pi_1(L(p, q)) \cong \mathbb{Z}/p$, (see [**14**, p. 234]). Thus the unit tangent bundle can be embedded into S^3 if and only if there exists an integer c such that $k + n - knc = \pm 1$, and this can happen only for the case $(2, 3)$ of the modular surface (unless k or n equals 1, but then we have less than two cone points).

Adding more singular fibers can never result in S^3 (see [**15**]). Gluing in a 3-manifold with boundary which is not a Seifert fiber space surely cannot result in S^3, as this makes the torus on which the two manifolds are glued upon an essential torus in the resulting manifold (while S^3 contains no essential torus). □

3.4. *Defining the vector field $\mathcal{V}$.* Our next goal is to obtain a homeomorphism from pointers on the orbifold into any of the relevant lens spaces computed above. We will now assume that $n = 2$, and we do this in two steps. The first consists of defining a particular vector field $\mathcal{V}$ on the orbifold minus a neighborhood of the cone points (in the present section). This gives an embedding of its domain, which is a pair of pants, into the unit tangent bundle. The second consists of completing this embedding to the different possible embeddings of $UT\mathcal{O}_{(n,k)}$ into lens spaces (in the two following sections). The completion is obtained by first gluing in the missing cone point neighborhoods, then gluing in the torus corresponding to the cusp. The last gluing can be done in countably many different ways, according to the Euler number of the resulting closed 3-manifold.

We next define a vector field $\mathcal{V}$ on the orbifold with some small neighborhoods of the cone points removed as in Figure 7: take the orbifold by a homeomorphism to the unit 2-sphere punctured at the north pole, taking the cusp to the north pole and the k-cone point to the south pole. Pull back the vector field pointing west at each point. This cannot define

https://doi.org/10.1017/etds.2012.132 Published online by Cambridge University Press

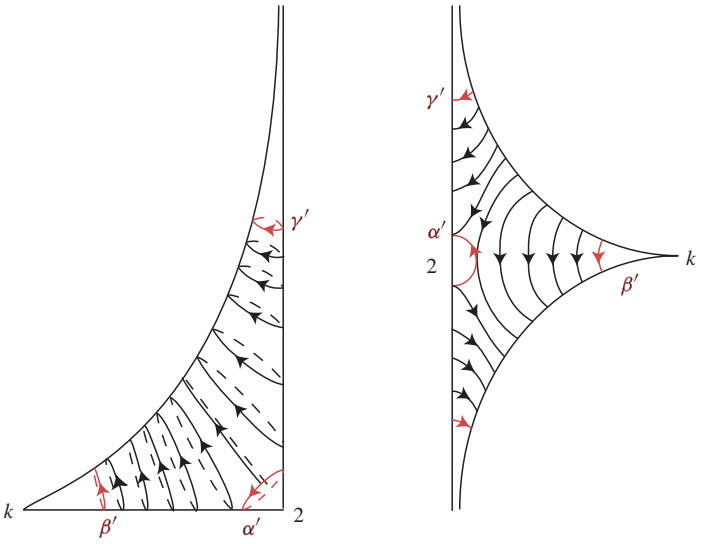


FIGURE 7. The vector field $\mathcal{V}$ over $\mathcal{O}_{(2,k)}$, shown both on the orbifold and on a fundamental domain.

a vector field on the orbifold including the neighborhood of the 2-cone point, as can be seen from Figure 7. Thus the domain of the vector field is a pair of pants, which we denote by A.

Another way of viewing the vector field $\mathcal{V}$ is as the image of an embedding of A into $UT\mathcal{O}_{(2,k)}$, taking each point of A to the pointer based at this point, with the direction given by the vector field at this point. The embedding has the following properties.

(1) Every fiber in the Seifert fibration of $UT\mathcal{O}_{(2,k)}$ away from the singular fibers intersects $\mathcal{V}$ once, since each fiber consists of the circle of directions at a point, and $\mathcal{V}$ chooses one of these directions. Hence $\mathcal{V}$ is a punctured orbit surface for the Seifert fiber space $UT\mathcal{O}_{(2,k)}$, and, in particular, its boundary curves α', β' and γ', lying respectively on the boundary tori for α, β and the cusp, are crossing curves, that is, cross each regular fiber on the boundary exactly once.

(2) As can be seen in Figure 7, one boundary component β' of $\mathcal{V}$ is a small loop around the k-cone point with its tangent vectors, hence is isotopic to the singular fiber β. This means that on a torus which is the boundary of a tubular neighborhood of the k-singular fiber, β' is homologous to a longitude plus x meridians for some $x \in \mathbb{Z}$. A regular fiber on this torus is a $(k, 1)$ curve, and by property (1), it intersects β' exactly once. Thus, x must be trivial and β' is simply isotopic to a longitude $(1, 0)$ on this torus. This uniquely determines the way to glue in the $(k, 1)$ singular torus, that is, determine the way to complete the embedding to the β neighborhood.

(3) Considering Figure 7 again, the boundary component α' of $\mathcal{V}$ is isotopic to a small loop around the 2-cone point with a direction rotating relative to its tangent vectors by one full rotation (clockwise). Hence, on the boundary torus of a tubular neighborhood of the 2-singular fiber, α' is homologous to a longitude $(1, 0)$ minus a regular fiber (which is a $(2, 1)$ curve on this torus), plus some number of meridians.

https://doi.org/10.1017/etds.2012.132 Published online by Cambridge University Press

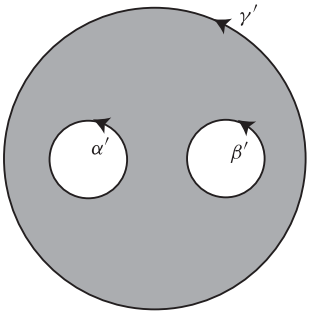


FIGURE 8. The vector field $\mathcal{V}$ is a subset of $UT\mathcal{O}_{(2,k)}$ homeomorphic to a pair of pants with boundaries as above.

Thus $\alpha' \cong (-1, y)$ for some $y \in \mathbb{Z}$. Together with property (1), this yields that α' is isotopic to either minus a longitude $(-1, 0)$ or a $(-1, -1)$ curve. The second option turns out to be the correct one, as will be computed below.

(4) The third boundary component γ' of the surface is isotopic to a small loop around the cusp together with its tangent vectors.

3.5. *The Euler number.* We now turn to the second step in explaining the embedding of $UT\mathcal{O}_{(2,k)}$ into the lens spaces. This step consists of explicating the gluing of the missing tori. To begin with, let us note the following conclusion from our previous discussion.

LEMMA 3.5. *All manifolds into which $UT\mathcal{O}_{(n,k)}$ embeds without adding a singular fiber are the Seifert fiber spaces*

$$M = \{O, o, 0|b; (k, 1), (n, 1)\}, \quad b \in \mathbb{Z}.$$

Proof. This follows since the pair of pants is orientable, unit tangent bundles are always orientable [**16**], $UT\mathcal{O}_{(n,k)}$ has two singular fibers, and we computed the invariants $(k, 1)$ and $(n, 1)$ of the two singular tori. □

Recall that any gluing matrix $M_{n,k,c}$ determines an embedding into a specific lens space M and M can be computed directly from the matrix.

We now relate the matrix to the Euler number of M. This will determine two things: which of the two possibilities for the coordinates of α' above is the correct one, enabling us to glue in the α neighborhood; and the relation between the parameter $c \in \mathbb{Z}$ of the gluing matrix and the Euler number $b \in \mathbb{Z}$ of the lens space.

The Euler number b is determined as follows. An abstract punctured orbit surface, in our case a pair of pants, is taken together with its (trivial) unit tangent bundle. A fibered torus with the correct invariants is glued into two holes in the pants, so the boundary of the pair of pants is a crossing curve for these tori. These are the neighborhoods of the singular fibers. Finally, to close the manifold a torus is glued into the third hole in the pair of pants, so that the meridian μ is glued to the curve $\gamma' - b \cdot f$ where γ' is the remaining boundary component of the pair of pants.

In our case γ' is a crossing curve (see §3.2), hence one can choose the longitude λ to be isotopic to a fiber f. Thus for M with Euler number b, $\gamma' \cong \mu + b \cdot \lambda$.

https://doi.org/10.1017/etds.2012.132 Published online by Cambridge University Press

Cut the pair of pants determined by the vector field along some curve δ connecting the γ' boundary to the β' boundary component. This yields two copies of the path δ on the boundary of the resulting annulus. Now attach a narrow rectangle to the annulus, with each of its shorter edges glued to one of the copies of δ, so that in between it goes $-b$ times in the direction of the fibers above δ. This yields a new pair of pants, while taking $\gamma' \cong \mu + b \cdot f$ to $\tilde{\gamma}' \cong \mu$. Hence, one boundary component of the new pair of pants is a boundary of an embedded disk. It thus follows that one can remove that boundary component and arrive at an embedded annulus A, with two boundaries: α' and $\beta' - b \cdot f$. Hence, α' can be isotoped to $-\beta' + b \cdot f$.

The matrix $M_{k,2,c}$ computed before takes the curve $\binom{-1}{-1}$ in the (2, 1) torus to the curve

$$\begin{pmatrix} -1 \\ 0 \end{pmatrix} + (c-1) \begin{pmatrix} k \\ 1 \end{pmatrix} = -\beta' + (c-1) \cdot f$$

in the $(k, 1)$ torus. This decomposition cannot be achieved with the other possible form for α'.

This yields

$$\alpha' = \begin{pmatrix} -1 \\ -1 \end{pmatrix},$$

$$b = c - 1,$$

completing the embedding determined by $\mathcal{V}$.

Remark. The complement of the image of the embeddings of $UT\mathcal{O}_{(n,k)}$ into lens spaces discussed before is a solid fibered torus. This torus is a regular neighborhood of any one of its fibers, that is, the image of the unit tangent bundle is the complement of a regular fiber in the lens space. Denote this fiber by ξ. The missing fiber, or 'missing knot' ξ, plays the same role as the trefoil for the modular flow.

3.6. *Interpreting the embedding.* We next make the embedding much more explicit: for any given pointer in $UT\mathcal{O}_{(n,k)}$ we will be able to identify its image in the lens space.

Recall that each of the relevant lens spaces is the union of a $(k, 1)$ and a (2, 1) torus. Take the $(k, 1)$ torus to be a very small neighborhood of the singular fiber β so that β' is on its boundary. It then follows that the (2, 1) torus contains the rest of $UT\mathcal{O}_{(n,k)}$, and in particular the vector field $\mathcal{V}$. We denote the (2, 1) torus by T_2 and take this torus to be oriented in the usual way, so that the orientation of the meridian followed by the orientation of the longitude gives the orientation of $\partial(T_2)$. The missing fiber ξ corresponding to the cusp is then a regular fiber in the interior of this torus (and not on its boundary as before).

We determined the coordinates of the boundary curves α', β' and γ' of the vector field. The coordinates are given each on the boundary tori which are the neighborhoods of α, β or ξ. Any two fixed boundary curves determine the pair of pants up to isotopy (see Seifert [**15**, p. 44]). Hence, it suffices that we identify one such pair of pants in the (2,1) torus, in order to identify $\mathcal{V}$.

We now describe such a pair of pants for the case $b = 0$. For this case $\gamma' \cong \mu$ is a meridian and so when filling in μ with a disk one gets an annulus intersecting ξ

https://doi.org/10.1017/etds.2012.132 Published online by Cambridge University Press

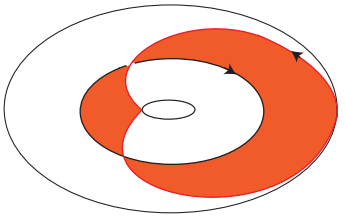


FIGURE 9. Two of the boundaries of the pair of pants corresponding to the vector field, the third being the puncture by the missing fiber ξ.

transversally. This corresponds to gluing the tori comprising the lens space by the matrix $M_{k,2,1}$ (since $c = 1 - b$). We represent the (2, 1) solid torus without a neighborhood of its core α as a union of concentric tori. Consider a $(-1, -1)$ curve on any one of these concentric tori. It intersects any (2, 1) fiber once. As we saw in §3.5, α' is a $(-1, -1)$ curve, and hence there is an annulus connecting a $(-1, -1)$ curve δ on the inner boundary of the torus T_2 to α', through $(-1, -1)$ curves on each of the concentric tori. The curve ξ appears in T_2 as a (2, 1) curve on one of the concentric tori and therefore will intersect this annulus transversally at a point. Thus, by puncturing the annulus at that point we arrive at the desired pair of pants. This follows from uniqueness since the punctured annulus has the desired boundaries α' and γ'. It follows that the pair of pants also has β' as a boundary, and indeed, one can easily check that the $M_{k,2,1}$ matrix takes $-\delta$ to β':

$$\begin{pmatrix} k-1 & 2-k \\ 1 & -1 \end{pmatrix} \begin{pmatrix} 1 \\ 1 \end{pmatrix} = \begin{pmatrix} 1 \\ 0 \end{pmatrix} = \beta'.$$

We continue our analysis of the embedding (which is determined up to isotopy) from $UTO_{(2,k)}$ into the lens space, focusing on embedding the complement of small neighborhoods of the singular fibers into T_2.

To begin with, our discussion in the previous section shows that the pair of pants described above (and depicted in Figure 9) is the image of all pointers comprising the vector field. Each pointer can be rotated by any angle while fixing its base point. By rotating all pointers of the vector field by the same angle at the same time we get an isotopy of the entire pair of pants $\mathcal{V}$. Of course, when the angle is 2π we retrieve $\mathcal{V}$ once again, as in Figure 10. Naturally, the intermediate punctured orbit surfaces all have the same Seifert invariants and thus are determined by $(-1, -1)$ curves.

The set of these pairs of pants is determined up to isotopy. Recall also that a counterclockwise rotation corresponds to flowing along the fibers in the positive direction.

This yields a concrete mapping $(p, \theta) \mapsto T_2$ as desired, where θ is the angle relative to the vector field.

4. *Templates*

4.1. *The Birman–Williams theorem* [**4, 8**].

Definition 4.1. A *template* is a compact branched two-manifold with boundary and a smooth expanding semi-flow built from a finite number of branch line charts, as in Figure 11.

https://doi.org/10.1017/etds.2012.132 Published online by Cambridge University Press

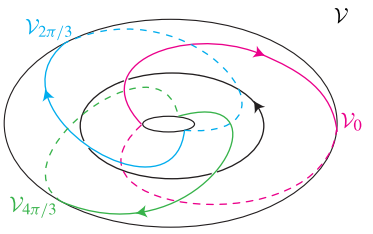


FIGURE 10. The boundary curve near β for three isotopic pairs of pants depicted in the torus T_2. Each pair of pants has another parallel boundary curve near α, which is the core of the torus. The third boundary component is a puncture by ξ . The curve marked $\mathcal{V}_0$ is the boundary of the original vector field $\mathcal{V}$. Every point travels along its fiber as one rotates the vector field counterclockwise, yielding the other pairs of pants.

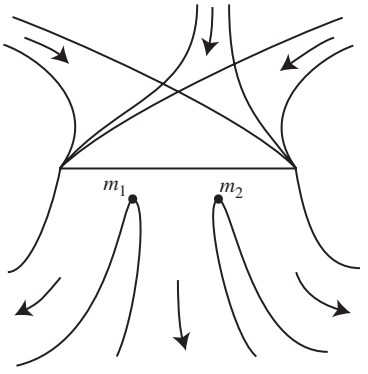


FIGURE 11. A branch line chart.

We now formulate the following fundamental fact, which underlies our discussion.

THEOREM 4.1. (Birman and Williams [**4, 8**]) *Given a flow ϕ_t on a three-manifold M having a hyperbolic chain-recurrent set, the link of periodic orbits $\mathcal{L}_\phi$ is in bijective correspondence with the link of periodic orbits $\mathcal{L}_\mathcal{T}$ on a particular embedded template $\mathcal{T} \subset M$. On any finite sublink, this correspondence is via ambient isotopy.*

In our case of geodesic flows on hyperbolic orbifolds, the chain-recurrent set equals the recurrent set, and this set is the closure of the set of closed geodesics. The recurrent set in this case, like the entire system, is always hyperbolic due to the divergence of geodesics in $\mathbb{H}$: hyperbolicity means that transversal to the direction of the flow there is an expanding direction and a contracting direction. These two directions are given by the horocycles, as explained in §2.2 for the geodesic flow on the hyperbolic plane. Since hyperbolicity is a local property, it descends to the quotients of the system, the flows on hyperbolic surfaces and orbifolds. Therefore by Theorem 4.1 there exists a template for the flow on any hyperbolic orbifold.

The general method of obtaining a template consists of collapsing the stable manifolds of a suitable neighborhood of the (chain) recurrent set, resulting in a semi-flow on a two-dimensional system, which turns out to be a branched surface. The key fact about

https://doi.org/10.1017/etds.2012.132 Published online by Cambridge University Press

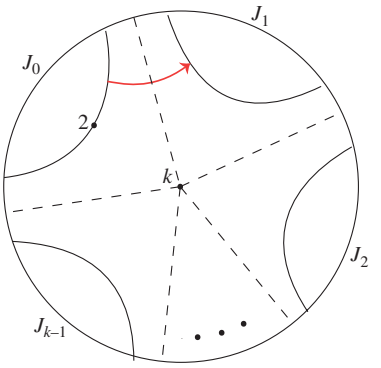


FIGURE 12. A cover of the fundamental domain.

this operation is that periodic orbits of the original flow remain unchanged, and are also periodic orbits of the new semi-flow. This consistency of orbits follows from the fact that different periodic orbits never belong to the same stable manifold. Birman and Williams then prove for this case that for the template resulting from the collapse, any finite set of periodic orbits can be carried on to it by an ambient isotopy.

Unfortunately, in general the stable manifolds will be dense and collapsing them would result in a non-Hausdorff space. Very informally, Birman and Williams overcome this by first 'separating' the stable manifolds by performing surgery on one or two periodic orbits, reducing the dimension of the recurrent set to one. Then, following Bowen, they describe a way to construct a 'nice' neighborhood of this one-dimensional set in which the stable manifolds can indeed be neatly collapsed, resulting in a template for the system. This process is not constructive for a general flow, and thus obtaining templates for different flows is an interesting problem, and templates have been obtained for a limited number of flows.

For hyperbolic geodesic flows the stable and unstable manifolds are known as in §2.2. We deal with the case of an orbifold with a cusp, for which the dimension of the basic set can always be reduced, as was noted by Ghys for the modular surface. By opening the cusp as in §2.4 one arrives at a system in which the recurrent set is the suspension flow on a Cantor set (in $\partial\mathbb{H}^2$) times itself, and so is one-dimensional. Thus, it follows from Birman and Williams that the stable direction can simply be collapsed on a suitable neighborhood of this set, which will be chosen in §4.2 to be exactly as in the modular case. At the same time, by the stability of the flow, the set of periodic orbits is unchanged by the cusp deformation. We refer the reader to [**10**] for the details, and a further discussion of this matter can be found in [**7**].

4.2. *Constructing a template for $\mathcal{O}_{(2,k)}$.* We now describe the embedded template in T_2. Following Ghys [**10**], consider the k-fold cover of the fundamental domain of $\mathcal{O}^d_{(2,k)}$ as in Figure 12, denoted D, where the generators of the group act by a rotation by π about x, and a rotation by $2\pi/k$ about y (see §2.4).

For every closed geodesic there is a lift passing through D, crossing from some segment of $\{J_0, \ldots, J_{k-1}\}$ to another. By using the rotational symmetry about y, any closed

https://doi.org/10.1017/etds.2012.132 Published online by Cambridge University Press

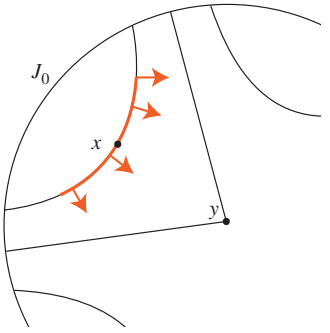


FIGURE 13. We choose this segment, with the perpendicular direction into the domain, as the branch line for our template.

geodesic has a lift with an arc emanating from J_0 and crossing the domain. At the endpoints of the arc, where the lift leaves D, we again use the rotation about y and then the rotation about x to identify each endpoint with a starting point of another arc. Hence these arcs contain the recurrent set of the geodesic flow.

We can choose the segment along the boundary of the fundamental domain (depicted in Figure 13) with perpendicular direction vectors into the domain, as a single branch line for the template.

For a general geodesic that is not necessarily perpendicular when entering the domain, we can always choose a different point along the stable manifold of the entry point of the geodesic, and arrive at a geodesic that is perpendicular at its entry point. Recall that the stable manifold is the horocycle corresponding to the starting point at infinity (on J_0) of the geodesic, with the direction vectors perpendicular to the horocycle pointing away from the starting point. If the geodesic is already perpendicular at the entry point, the horocycle and the boundary of the domain are tangent, and we do nothing. Otherwise, the horocycle crosses the boundary transversally and enters the domain. The horocycle returns to J_0, and therefore must cross the boundary again at some other point. By looking at the geodesics perpendicular to the horocycle at each point between the two crossing points, we see that the angle they create with the boundary changes monotonically, and must pass through $\pi/2$. Hence, by the mean value theorem there exists a point as required. Thus, the chosen branch line contains a point of the equivalence class of every arc passing in D, and so represents all the recurrent dynamics.

Using the embedding derived in the previous section, we are able to embed the branch line (for any k) in T_2. One half of the branch line is contained in $\mathcal{V}$, while the other half in $\mathcal{V}_\pi$. Hence, the branch line is embedded as shown in Figure 15 for the particular case (2, 5).

Our template has $k-1$ bands emanating from the branch line, each containing the arcs in D emanating from J_0 and reaching the same segment J_i. The bands each return to the branch line by using the group symmetries as above. These bands are called ears, and we denote the ear reaching J_i by E_i. Each ear stretches across the entire branch line when

https://doi.org/10.1017/etds.2012.132 Published online by Cambridge University Press

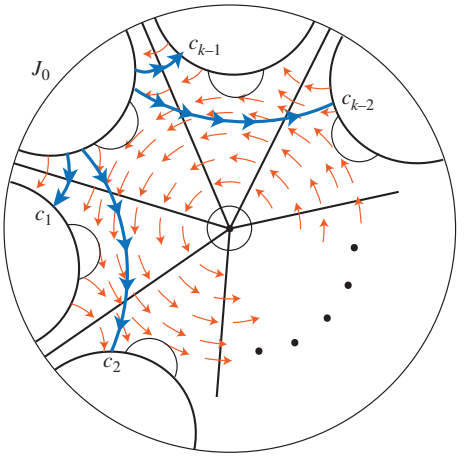


FIGURE 14. Comparing the vector field $\mathcal{V}$ to the closed geodesics which are the cores for the template ears.

returning to it, as any starting point can be obtained by the symmetries, from endpoints at any segment $J_1, \ldots, J_{k-1}$. Denote the core of E_i by c_i, where c_i is the unique closed geodesic contained in the ear.

To understand the embedding of the template we have to understand two things: the embedding of each core, and the twisting of the ear about its core. We begin with embedding the ear cores. To this end consider Figure 14 comparing the tangent vectors to each of the ear cores to the vector field $\mathcal{V}$. Here we draw $\mathcal{V}$ by taking the k-fold cover of $\mathcal{V}$ as depicted in Figure 7.

Next, we must again consider Figure 10, which sets the correspondence between each angle relative to $\mathcal{V}$ and a specific pair of pants in T_2. This yields the embedding of the cores into T_2, and we now work out one example in detail. The resulting embedded cores, together with the branch line, are sketched for the case (2, 5) in Figure 15. We go through the process of obtaining this figure.

The cores c_1 and c_4 (and in general c_{p-1}) are easily identified. Their projections to the orbifold are small loops around the cusp, and the tangent direction to c_1 coincides everywhere with $\mathcal{V}$, while the tangent direction to c_{p-1} is opposite to $\mathcal{V}$ at every point. Thus they are equal to the cusp boundary component of $\mathcal{V}_0$ and $\mathcal{V}_\pi$, respectively. These are determined (both their position and orientation) by completing the boundaries given in Figure 10 to pairs of pants (that is, to annuli punctured by ξ). The next two cores can be understood by decomposing their projections on the orbifold as follows. First they follow a loop around the cusp, further away from the cusp relative to the first loops, then a loop around the 2-cone point, then again a loop around the cusp. At the same time, they travel back and forth through the different pairs of pants, as their angle relative to $\mathcal{V}$ increases, then decreases, and vice versa, as in Figure 14. This is enough for understanding the four cores of the (2, 5) case, given in Figure 15, or for the two first and two last cores in any $(2, k)$ template, $k > 3$.

https://doi.org/10.1017/etds.2012.132 Published online by Cambridge University Press

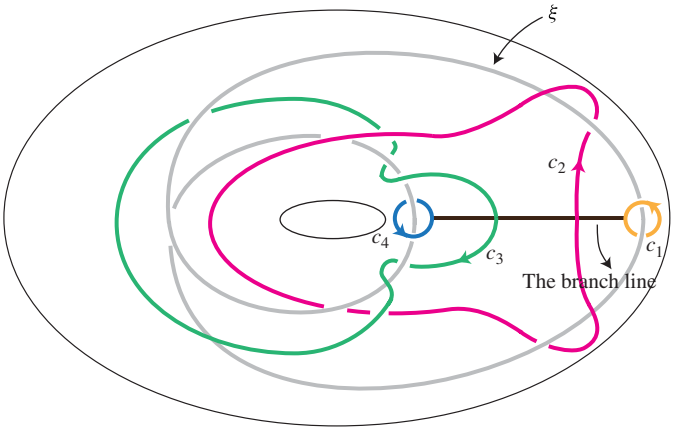


FIGURE 15. The cores of the four ears of the (2, 5) case in $T_2\backslash\xi$.

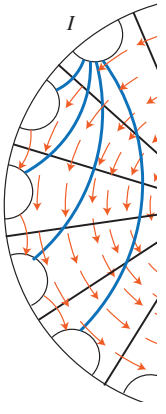


FIGURE 16. Comparing the vector field to all the ear cores.

We now consider the next ears in a general $(2, k)$ template. The four first ear cores for any flow on $\mathcal{O}_{(2,k)}$ for $k \geq 9$ are given in Figure 16. We note two facts regarding these cores. Each subsequent core reaches a larger angle relative to the vector field before returning to the vector field direction. The core corresponding to the ear E_j has j parts, each isotopic to β', that is, a circle around the k-cone points, and each subsequent core is closer to the β' curve. These four first loops for any k are sketched, by the same method as for the to first (and last) ears above, in Figure 17.

We next compute for each ear the embedding of one orbit in addition to the core. This will determine the twists of each ear, and thus the template. A second orbit in the same ear is never closed, and so will have two parts. The first part is a geodesic segment: we choose a geodesic which emanates from the branch line perpendicularly to the boundary of the domain, very close to the closed geodesic, closer to the 2-cone point along the branch line. For this segment for any of the ears, we find it reaches a larger angle than the core relative

https://doi.org/10.1017/etds.2012.132 Published online by Cambridge University Press

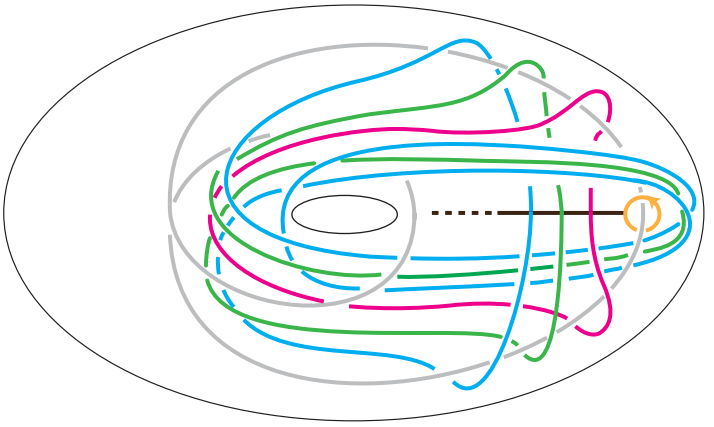


FIGURE 17. The first four cores for any $k \geq 9$.

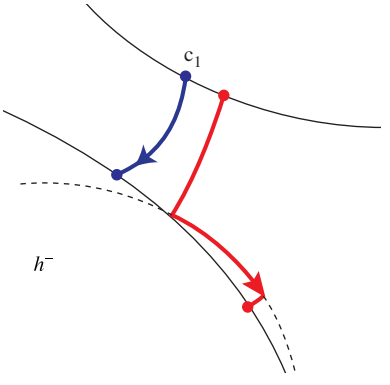


FIGURE 18. Drawing a second flow line in the first template ear.

to the vector field before returning to it, and is closer than the core to β'. This is shown in Figure 18 for the first ear. This means that this segment is in the direction of the next core (if it exists), and we can draw this segment in T_2 according to our embedding of the cores above.

When the above geodesic segment again reaches the boundary of the fundamental domain as in Figure 13, its direction is not perpendicular to the boundary. This means that in the unit tangent bundle this geodesic arc did not return to the branch line. The second part of the orbit will connect it to the branch line through segments of stable manifolds and geodesic segments, as explained above in general. In this case, by choosing a segment close enough to the closed geodesic, the second step can be done in one 'move'. This is sketched in Figure 18 for the first ear.

This is the last ingredient needed for determining the template completely, and is then done for each of the template ears. The resulting template is sketched in Figure 19 for the (2, 5) case.

https://doi.org/10.1017/etds.2012.132 Published online by Cambridge University Press

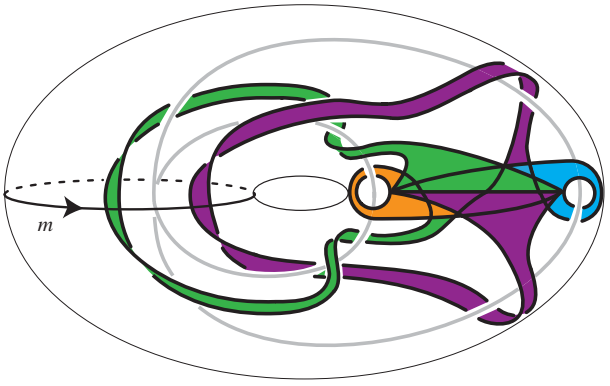


FIGURE 19. The template for the (2, 5) case.

Remark. Note that the linking number of any closed geodesic with the missing knot ξ is well-defined in any of the lens spaces, and can be easily read off the sequence of ears of the template through which the geodesic passes.

5. *A unified Hecke template*

Up to now it may seem that due to their complexity, and the number of ears which increases with k in these templates, it will be quite pointless to study them. In this section we obtain a single relatively simple template, containing all $(2, k)$ templates as subtemplates. Thus, by studying a single template, knot invariants may be obtained for all of the flows considered here at once.

We next analyze the structure of the template for a larger k. The four loops in Figure 17 can be isotoped to yield Figure 20. It is obvious that this is similar for the four last ears by symmetry, and that this generalizes to the next ears. It is true for all ears that for a second orbit starting closer to the middle of the branch line, the maximal angle from the vector field increases, while the image approaches β'. The number of times the geodesic encircles the k-cone point increases by one when passing from one ear to the next. Thus, when one executes the same analysis for the twisting of the ears as in the $(2, 5)$ case by examining one more loop in each ear, one finds the additional ears can also be put beside each other exactly as in Figure 20.

The last step in our analysis is to glue the ears together along the sections of their boundaries, on which they run parallel to each other. Note, however, two ears can never be glued on their entire boundaries as they are of different homology types. In this way we obtain a template with a smaller number of ears, that actually does not increase with k. As can be seen from Figure 20, we have to add another branch line in the middle of the first loop, and the same is of course true for the last loop, as in Figure 21.

For each of the three branch lines we now have two ears arriving at it, but it is true only for the middle one that both ears cover it completely. We now address this last fact. Any ear E_i, in any of the original templates we constructed above, starts at the central branch line, arrives at one of the side branch lines and then makes some journeys along

https://doi.org/10.1017/etds.2012.132 Published online by Cambridge University Press

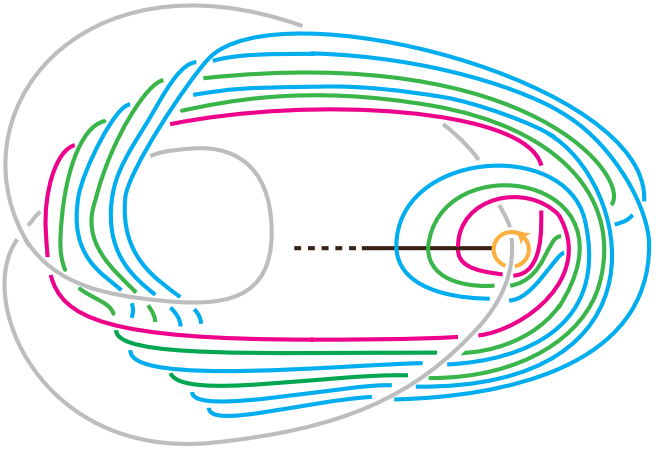


FIGURE 20. The first four template ears rearranged.

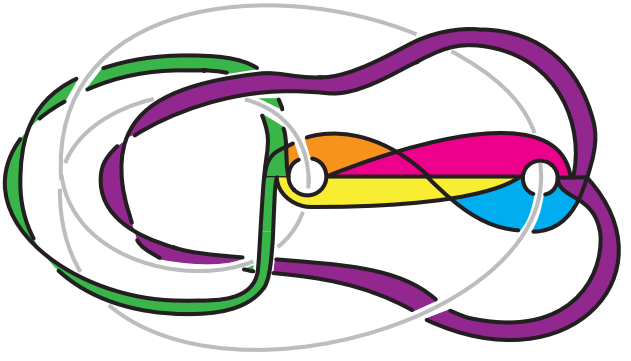


FIGURE 21. A template carrying any $(2, k)$ template as a subtemplate.

the core of T_2 (through one of the long ears in Figure 21, before returning to the central branch line). The number of journeys through the long ear equals $i - 1$ if $i < k - 1/2$, and $k - i - 1$ otherwise. Hence, to obtain the subset corresponding to a fixed k in the template in Figure 21, we note all flow lines in the longer ears existing already in the $(2, k)$ template cover the branch line, at their end point, only partly. Namely, they cover the part from which the shorter ear (the one returning to the central branch line) emanates, and some section from which the longer ear emanates, up to a point we denote by c from which after flowing through this longer ear $k - 1/2$ times, one arrives at the critical point of this branch line (that is, the flow line exits the template right afterwards). Thus, the maximal number of times an orbit of the subset can pass through one of the longer ears without arriving back at the central branch line is $k - 1/2$.

Then, for this set to satisfy the definition of a template, one has to propagate forward the right boundary point c of the long ear of the subtemplate (so that the ear covers the

https://doi.org/10.1017/etds.2012.132 Published online by Cambridge University Press

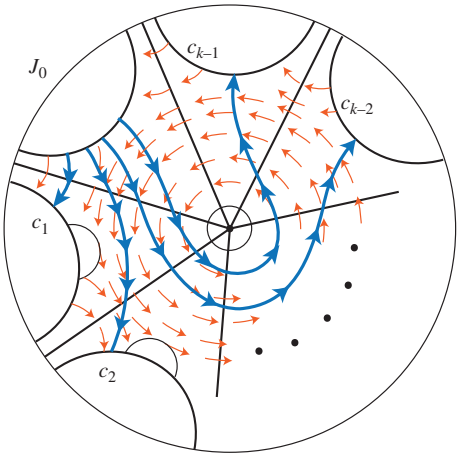


FIGURE 22. A different choice for the ear cores.

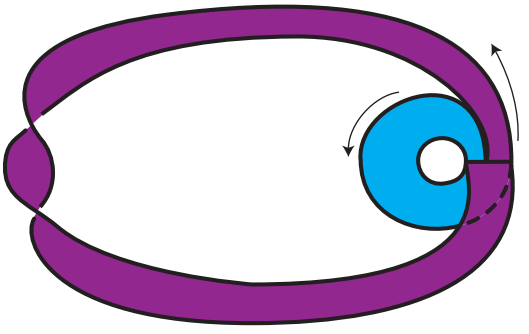


FIGURE 23. A different resulting universal template.

entire branch line), from the branch line through the template ears. This has to be done recursively a number of times, and will result in the original template we obtained for the $(2, k)$ case, with a number of ears increasing with k. Thus we have proved the following theorem.

THEOREM 5.1. *The template for the geodesic flow on the orbifold $\mathcal{O}_{(2,k)}$, for odd k, is a subtemplate of the template given in Figure 21, embedded in the* $(2, 1)$ *torus in the lens space* $L(k-2, 1)$.

We thank the referee for the following suggestion: one can also consider the cores of the template as curves going from the same side of the k-cone point as in Figure 22. It follows from the arguments above that these are indeed regular isotopic to the geodesic cores used before.

It is obvious that these arcs can be arranged so that the ones closer to β have a larger angle with $\mathcal{V}$, and that these isotopies can be made all at once for all the ear cores. Thus, it is also true here that the ears can be glued to each other on the sections of their

https://doi.org/10.1017/etds.2012.132 Published online by Cambridge University Press

boundaries which are homotopic. This results in a template in which every $(2, k)$ Hecke template appears as a subtemplate, which is shown in Figure 23. In this figure the Lorenz subtemplate is much less apparent, but one obtains a much simpler template. This last template is very similar to a Lorenz-like template as studied in [**17**], but the ear cores here are not null-homotopic.

Acknowledgements. I wish to thank Amos Nevo for suggesting this problem, and for his constant guidance and encouragement. Thanks are also due to Yoav Moriah for his contribution, Joan Birman and Robert Ghrist for their interest and advice, and the referee for some extremely useful comments.

References

[1] M. V. Berry. Quantum theory near the classical limit. *Highlights Phys. (SERC)* (1990), 50–51.
[2] J. Birman. Book review: Braid groups, ordering braids. *Bull. Amer. Math. Soc.* **48**(1) (2011), 137–146.
[3] J. Birman and R. F. Williams. Knotted periodic orbits in dynamical systems–I: Lorenz's equations. *Topology* **22**(1) (1983), 47–82.
[4] J. Birman and R. F. Williams. Knotted periodic orbits in dynamical systems-II: Knot holders for fibered knots. *Cont. Math.* **20** (1983), l–60.
[5] P. Cvitanovic. Dynamical averaging in terms of periodic orbits. *Physica D* **83** (1995), 109–123.
[6] P. Dehornoy. Les noeuds de Lorenz. *L'enseignement Math.* (2) **57** (2011), 211–280.
[7] P. Dehornoy. Geodesic flow, left-handedness, and templates. *Preprint*, 2011, arXiv:1112.6296.
[8] R. W. Ghrist, P. J. Holmes and M. C. Sullivan. *Knots and Links in Three-Dimensional Flows*. Princeton University Press, Princeton, NJ, 1997.
[9] R. W. Ghrist. Branched two-manifolds supporting all links. *Topology* **36** (1997), 423–448.
[10] E. Ghys. Knots and dynamics. *Proc. Int. Congress of Mathematicians*. Vol. 1. International Congress of Mathematicians, Zürich, 2007.
[11] D. Mackenzie. A new twist in knot theory. *What's Happening Math. Sci.* **7** (2009), 2–17.
[12] J. M. Montesinos. *Classical Tessellations and Three-Manifolds*. Springer, 1987.
[13] T. Pinsky. Primeness of Hecke knots, in preparation.
[14] D. Rolfsen. *Knots and Links*. American Mathematical Society, Providence, RI, 2003.
[15] H. Seifert. Topology of 3-dimensional fibered spaces. *Acta. Math.* **60** (1933), 147–288.
[16] N. Steenrod. *The Topology of Fiber Bundles*. Princeton University Press, Princeton, NJ, 1951.
[17] M. Sullivan. Prime decomposition of knots in Lorenz-like templates. *J. Knot Theory Ramifications* **2**(4) (1993), 453–462.
[18] M. Sullivan. Factoring families of positive knots on Lorenz-like templates. *J. Knot Theory Ramifications* **17**(10) (2008).
[19] V. V. Tsanov. Triangle groups, automorphic forms, and torus knots. *Preprint*, arXiv:1011.0461v2.
[20] M. Watkins. A short survey of lens spaces. Undergraduate dissertation, University of Kent at Canterbury, 1990.

https://doi.org/10.1017/etds.2012.132 Published online by Cambridge University Press